Supporting Information

Tuning the selectivity of bimetallic Cu electrocatalysts for CO_2 reduction using atomic layer deposition

Si Young Lee,‡[a] Julia D. Lenef,‡[b] Daniel O. Delgado Cornejo,[b] Alondra M. Ortiz-Ortiz,[a] Tao Ma [c], Timothy S. Arthur,[d] Charles A. Roberts,[d*] and Neil P. Dasgupta[ab]*

[a]*Department of Mechanical Engineering, University of Michigan, Ann Arbor, Michigan 48109 United States*

[b]*Department of Materials Science and Engineering, University of Michigan, Ann Arbor, Michigan 48109 United States*

[c]*Michigan Center for Materials Characterization, University of Michigan, Ann Arbor, MI 48109, USA*

[d]*Toyota Research Institute of North America, Ann Arbor, Michigan 48105, United States*

‡These authors contributed equally

*Email: ndasgupt@umich.edu, charles.roberts@toyota.com

Experimental Methods

Cu-Zn bimetallic catalyst synthesis

Copper and zinc nanoparticle alloys were synthesized with (PE)ALD on carbon GDEs (Sigracet 22BB from Fuel Cell Store) and planar Si substrates. The GDEs are comprised of (1) a top microporous layer (MPL) which consists of a mixture of graphitic carbon black and ~20-25% PTFE, and (2) a

macroporous backing layer with 5% PTFE. Each (PE)ALD experiment was performed using the Veeco ALD Fiji system. To form metallic Cu, a 300 W H_2 plasma was utilized as the reductant with a copper(I) N,N′-disec-butylacetamidinate ([Cu(sBu-amd)]2) as the metal precursor. To form a Cu-Zn bimetallic catalyst, 57 supercycles of 1 Zn: 9 Cu (570 total cycles) were performed. One supercycle begins with a thermal ZnO deposition step, which consists of 0.06 s pulse of diethylzinc (DEZ), and 0.065 s of water separated by 10 s purge steps for each half-reaction. This is followed by nine plasma-enhanced Cu deposition steps, which include a 3 s precursor pulse and an H_2 plasma exposure time of 10 s with 8 s purge steps. The identical process was repeated for the 7 supercycles of 1 Zn: 81 Cu alloy recipe (574 total cycles). The ALD experiments for Cu PEALD catalyst and Cu-Zn alloy bimetallic catalyst, Ar was used as the carrier gas at a flow rate of 110 sccm. The deposition temperature was maintained at 185 ℃ and the Cu precursor was held at 110 ℃ in a bubbler with DEZ at room temperature. Our previous work has confirmed the Cu growth rate on Si is ~0.2 A/cycle[1] and ZnO has a growth rate of 1.83 A/cycle at 200 C, which should closely match that of 185 C also within the ALD temperature growth window.

To overcoat the Cu PEALD catalyst synthesized on GDE with ZnO and Al_2O_3, DEZ and trimethylaluminum (TMA) precursors were used, respectively, in a custom-built ALD system in the laboratory.[2] Both reactions were carried out at a chamber temperature of 150°C, with a base pressure of 0.1 torr. The DEZ and TMA precursors were pulsed for 0.05 seconds, and DI water was pulsed for 0.1 seconds. Each pulse was followed by a 30-second Ar purge.

Materials Characterization

To evaluate the crystal phase, grazing-incidence X-ray diffraction (GIXRD) was performed using a Rigaku SmartLab X-ray diffractometer with a 2θ range of 20° to 70°. The incident angle was maintained at 0.5°. Scanning electron microscopy (SEM) was performed on a TESCAN MIRA3 FEG SEM with a 15 kV beam voltage. A Thermo-Fisher Helios Dual-Beam FIB/SEM was also used at 2 kV as the beam voltage also used. Surface chemical analysis was performed using a Kratos Axis Ultra X-ray photoelectron spectroscopy (XPS).

Measurements were taken using a monochromatic Al source (10 mA, 12 kV), and 160 and 20 eV were the pass energies for the survey scans and the core scans, respectively. The spot size was 700 μm by 300 μm and calibration was performed to the C–C component of C 1s peak at 284.8 eV. Scanning transmission electron microscopy (STEM) was performed using a Thermo Fisher Scientific Spectra 300 probe-corrected STEM operated at 300 kV. High-angle annular dark-field (HAADF) images were acquired with a detection range of 62–200 mrad. Energy-dispersive X-ray spectroscopy (EDS) mapping was carried out with the Dual-X EDS system with a probe current of ~300 pA.

Electrochemical Analysis

Electrochemical CO_2RR (ECR) experiments were performed in an H-cell configuration. For the H-cell tests, the geometric area of the working electrode was masked to be 0.5 cm^2. An Ag/AgCl (BASi, 3 M NaCl) and a graphite rod were used for a reference and a counter electrode, respectively. In the custom-designed polyether ether ketone (PEEK) H-cell, an anion exchange membrane (AEM; Fumasep, FAA-PK-75) was used to separate the cathode and anode compartment. 0.1 M $KHCO_3$ (Sigma-Aldrich, >99.95%) was prepared by purging with CO_2 (99.999%) for at least 30 minutes. CO_2-saturated 0.1 M $KHCO_3$ was used for the electrolyte and continuously flowed with CO_2 at a flow rate of 20 sccm during ECR. The ECR was measured by chronoamperometry using a potentiostat (Biologic, SP-200) and all potentials were given vs. the reversible hydrogen electrode (RHE) after calculated iR compensation measuring the potentiostatic electrochemical impedance spectroscopy (EIS).

Electrochemical Methods for iR Compensation

Post-iR correction is performed using solution resistance (R_u) from PEIS and the I_{avg} after each chronoamperometry (CA) experiment at a set voltage using Equation 1:

$$V_{RHE} = V_{app\ (vs.\ Ref)} + (0.059 \times pH) + 0.209\ (Ag/AgCl) - (R_u * I_{avg\ vs.\ Ref}) \quad [1] \quad (pH = 6.8)$$

In equation 1, V_{RHE} is the desired potential, 0.059 is related to Faraday's constant at the standard pressure and temperature, 0.2 V is the Ag/AgCl reference potential and R_u is the PEIS fitted solution resistance at -1 V vs Ref. Finally, $I_{avg\ vs.\ Ref}$ is the average current for the partial duration of the CA experiment, typically separated into 15 min intervals to match the GC sampling time. The pH of the solution is maintained at approximately 6.8.

Product Analysis

The gaseous products (H_2, CO, CH_4, C_2H_4, and C_2H_6) were detected using gas chromatography (GC; Agilent, 8890) - equipped w ith a ShinCarbonST packed column and Ar (99.999%) carrier gas. This GC system uses a six-port valve to sample gas, and it is connected online with the H-Cell to perform sampling 4 times per hour, which is averaged over the collection periods. H_2 gas was detected by a thermal conductivity detector (TCD) and the other gases (CO, CH_4, C_2H_4, and C_2H_6) were passed through a methanizer and detected by a flame ionization detector (FID). The Faradaic efficiencies (FEs) of the gas products were obtained by calculating the ratio of partial current density ($i_{partial}$) to total current density (i_{total}). The value of $i_{partial}$ is calculated using Equation 1, where the variables represent ambient pressure (p_0, 1 atm), volume concentration detected by GC (V_p), the flow rate of gas (Q), ideal gas constant (R), temperature (T), the number of electrons required to produce one mole of product (n), and Faraday constant (F).

$$FE\ (\%) = i_{partial}/i_{total} \times 100 = (p_0 \times V_p \times Q \times nF/RT)/i_{total} \times 100 \quad [1]$$

Liquid product analysis was performed by extracting 1.0 mL of the electrolyte after the conclusion of each experiment. The each catalyst was sampled after 1 hour of reaction. Next, 0.45 mL of the extracted electrolyte was mixed with 0.05 mL of an internal standard solution that was composed of 10 mM dimethyl sulfoxide (DMSO, Sigma-Aldrich, 99.9%) and 50 mM phenol (Sigma-Aldrich 99.0–100.5%) in D_2O (Sigma-Aldrich, 99.9% atom % D). This liquid

sample solution was analyzed by ^{1}H nuclear magnetic resonance (NMR) spectroscopy (700 MHz, Varian, Vnmrs 700). The relative peak area of formate was determined using phenol and the relative peak area of other products was determined using DMSO. Water suppression by pre-saturation of the water peak was employed during data collection. All relative areas of liquid products were compared to the standard curves to quantify the concentration of each liquid product. The required Coulombs of charge to generate each liquid product was divided by the passed Coulombs of charge during chronoamperometry to calculate the Faradaic efficiency of the liquid products.

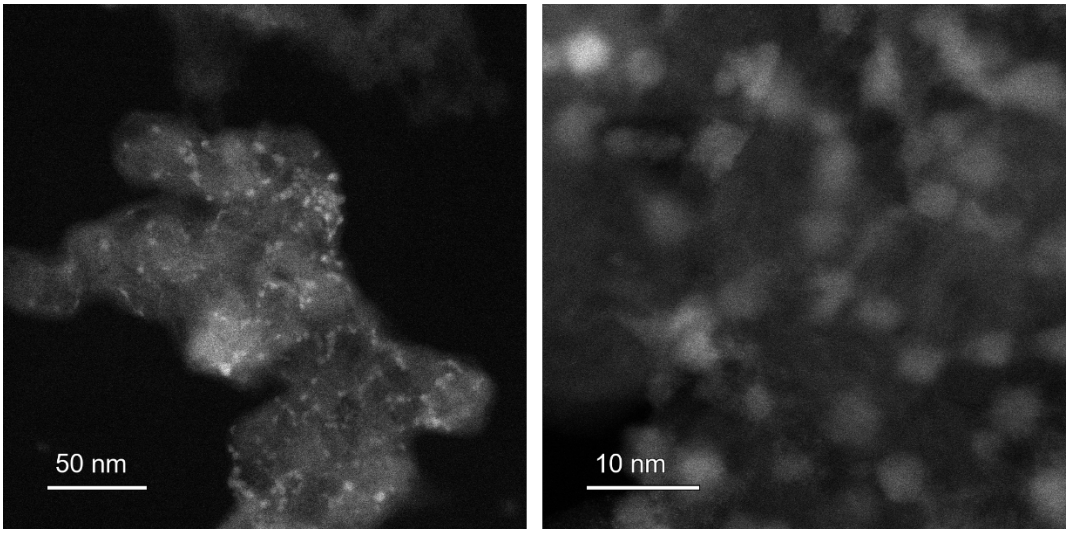

Figure S1. STEM-HAADF image of Cu PEALD and 3cycle ZnO ALD overcoating nanoparticles.

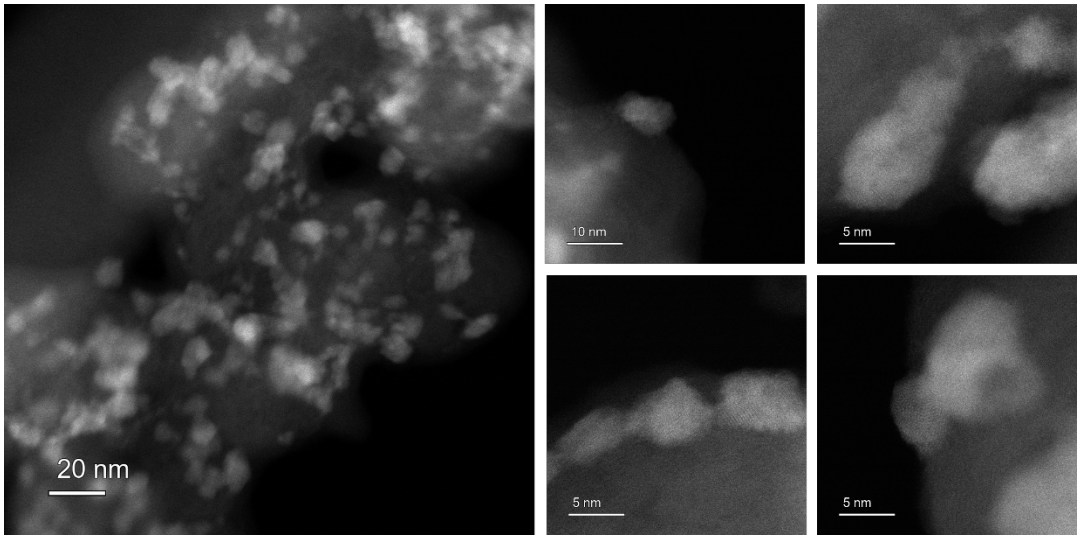

Figure S2. STEM-HAADF image of Cu-Zn 9:1 Supercycle sample nanoparticles.

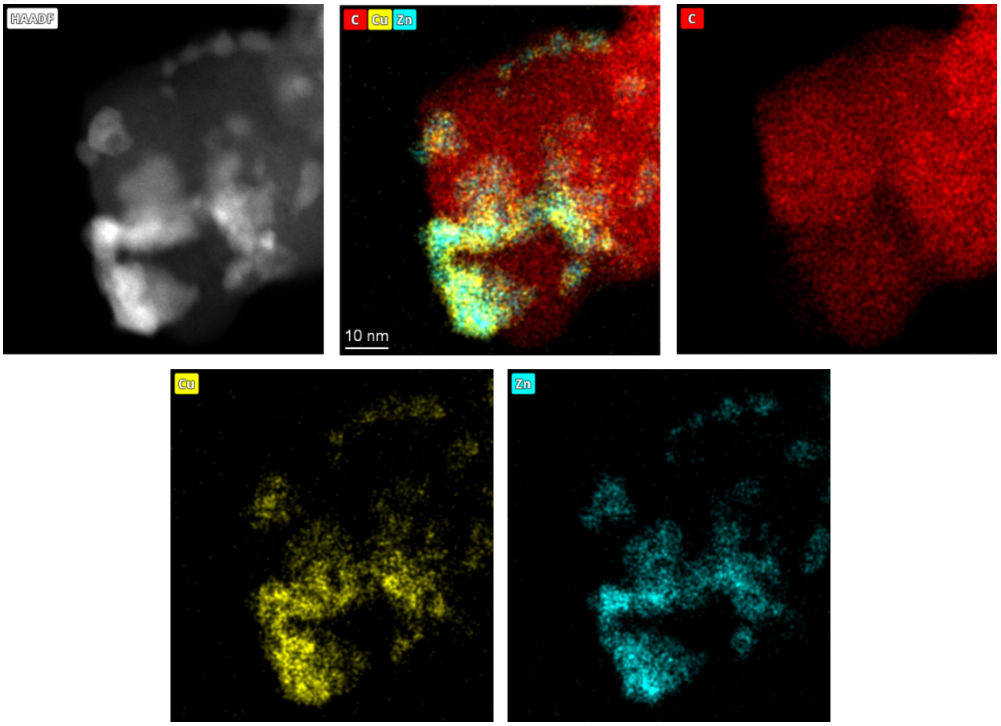

Figure S3. STEM-EDS mapping of Cu-Zn 9:1 Supercycle sample nanoparticles.

Table S1. The XPS survey scan results showing the elemental content for each different supercycle ratio of Cu-Zn alloy catalyst.

Element	Cu-Zn 9:1 supercycle (at %)	Cu-Zn 81:1 supercycle (at %)
Cu	6.63	4.4
Zn	6.66	1.67
C	66.2	72.75
O	6.4	8.01
F	13.5	11.98
N	0.7	1.18

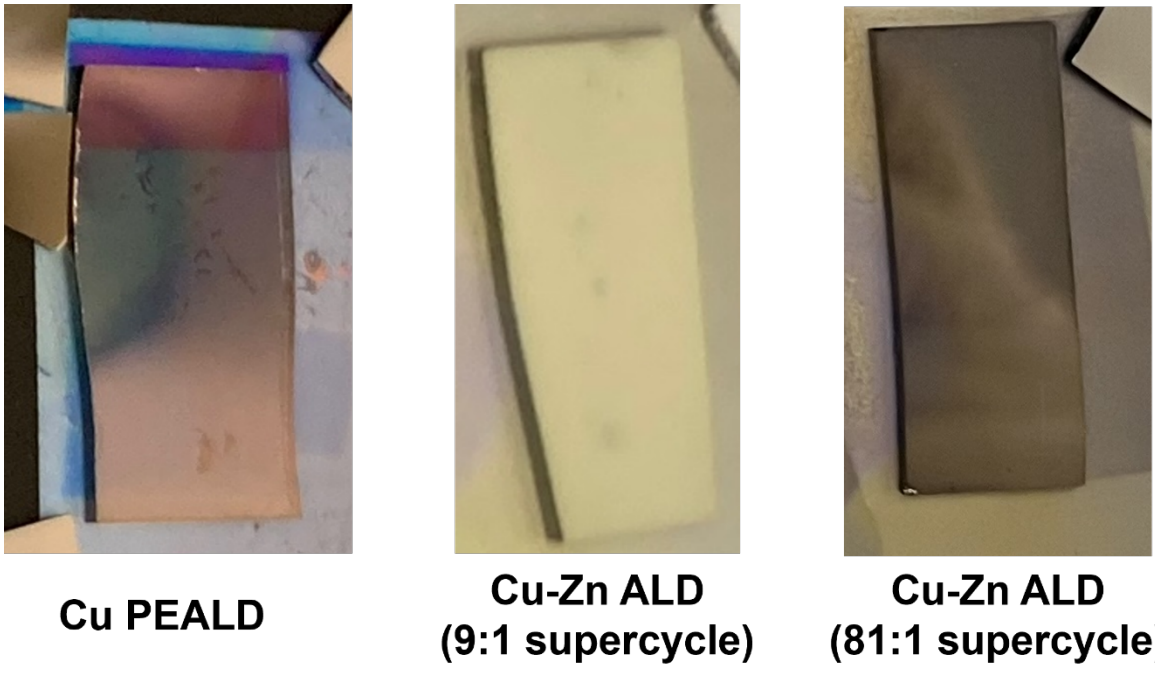

Figure S4. The colour difference between Cu PEALD catalyst and Cu-Zn supercycle alloy catalysts on glass substrates.

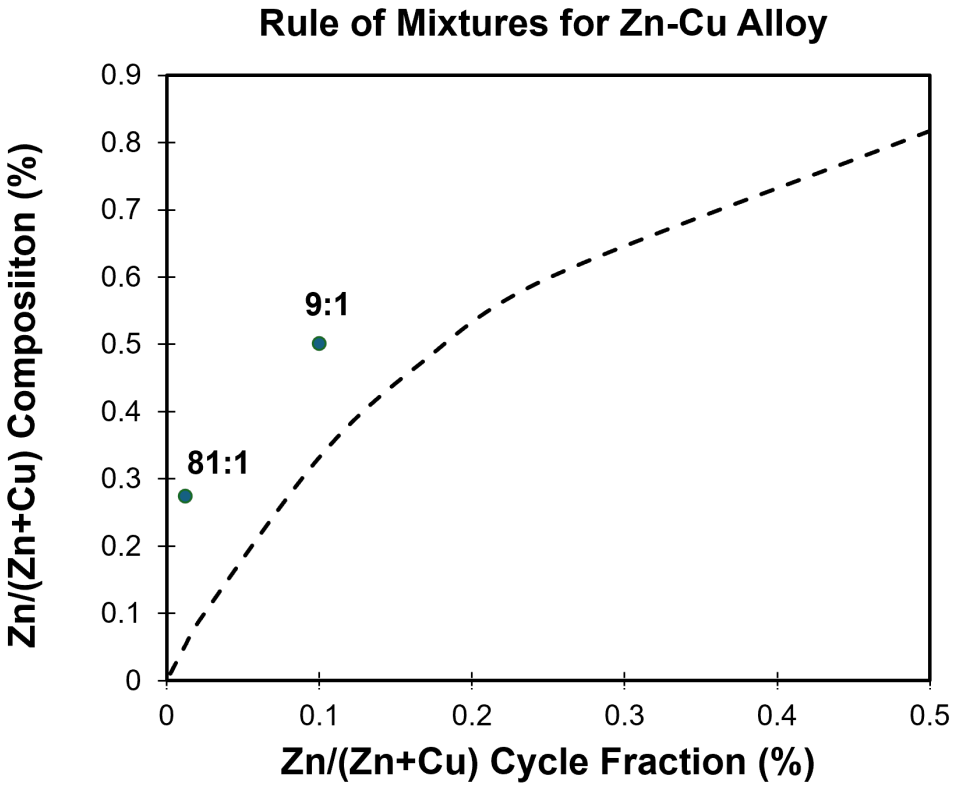

Figure S5. The theoretical rule of mixture graph between Cu and Zn fractions (dash line). The dots indicating 9:1 and 81:1 represent the actual Cu-Zn ratios observed by XPS survey scan.

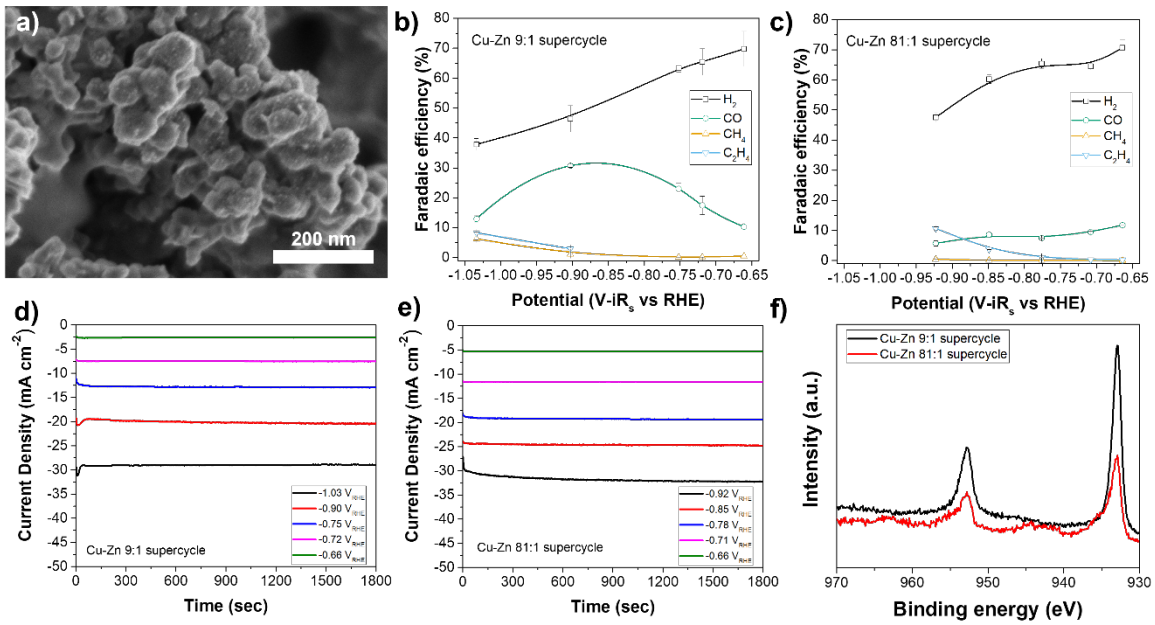

Figure S6. The SEM, ECR and Cu 2p XPS core scan results of 81:1 and 9:1 supercycle Cu-Zn catalysts. a) SEM image of Cu-Zn 81:1 supercycle catalyst on 22BB GDE substrate. b) Gaseous products FE results of potential dependence for Cu-Zn 9:1 supercycle catalyst. c) Gaseous products FE results of potential dependence for Cu-Zn 81:1 supercycle catalyst. d) Representative current density data of Cu-Zn 9:1 supercycle catalyst at different potential. e) Representative current density data of Cu-Zn 81:1 supercycle catalyst at different potential. f) Cu 2p XPS core scan spectrum for Cu-Zn 9:1 and Cu-Zn 81:1 supercycle catalysts.

According to the XPS Cu 2p core scan results, both 9:1 and 81:1 supercycle catalysts have similar binding energies at 932.9 eV (Fig S3f). The (002) XRD peak shift, however, was observed at a low

angle of 0.32 degrees for 81:1 catalyst and 0.96 degrees for 9:1 catalyst compared to Cu reference (Fig. S4). These results suggests that the difference in C_{2+} selectivity between the two catalysts may be affected by the lattice parameters of the alloy as well as the chemical state of the catalyst.

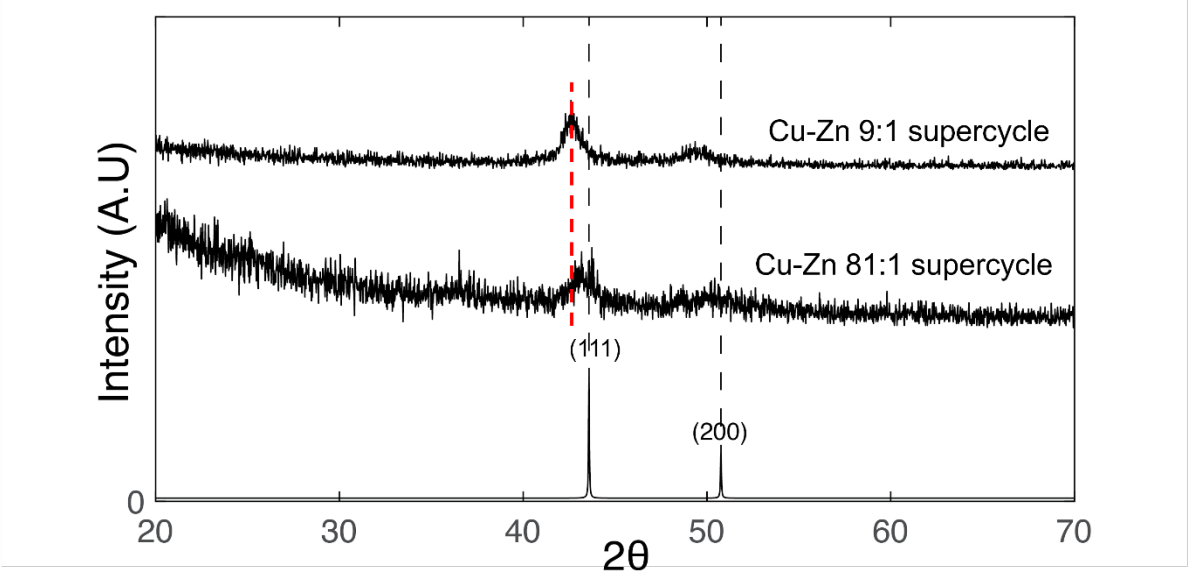

Figure S7. The XRD pattern of each Cu-Zn supercycle alloy catalyst. The bottom solid line represents the FCC Cu reference pattern (ICDS no: 15985). The black dash line indicates the peak centers of FCC Cu (111) and (200). The red dash line indicates the peak center of the Cu-Zn 9:1 supercycle catalyst for the (111) peak.

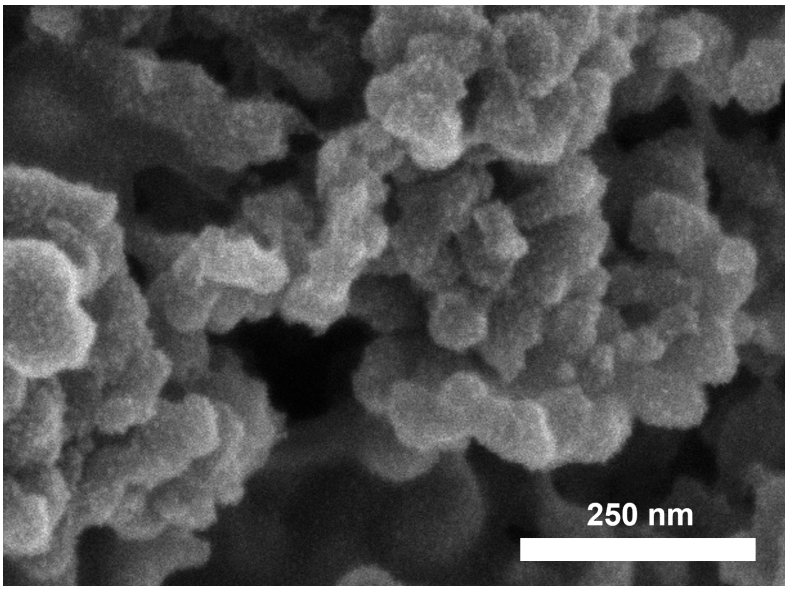

Figure S8. The SEM image after 3cycle ZnO ALD overcoating on a bare Cu PEALD catalyst.

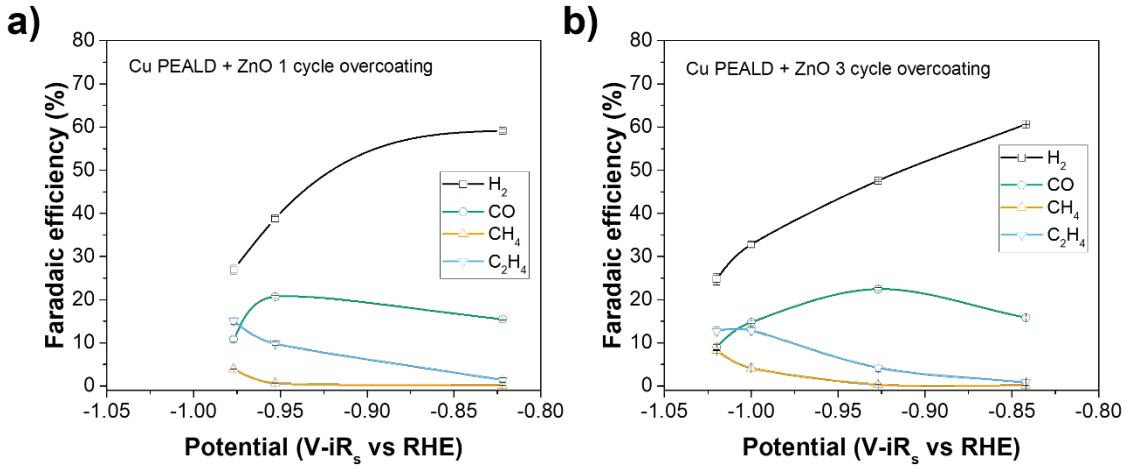

Figure S9. Potential-dependent gaseous product Faradaic efficiency of ZnO 1 cycle and 3 cycle overcoating on Cu PEALD catalysts. a) Gaseous product Faradaic efficiency of ZnO 1 cycle overcoating catalyst. b) Gaseous product Faradaic efficiency of ZnO 3 cycle overcoating catalyst.

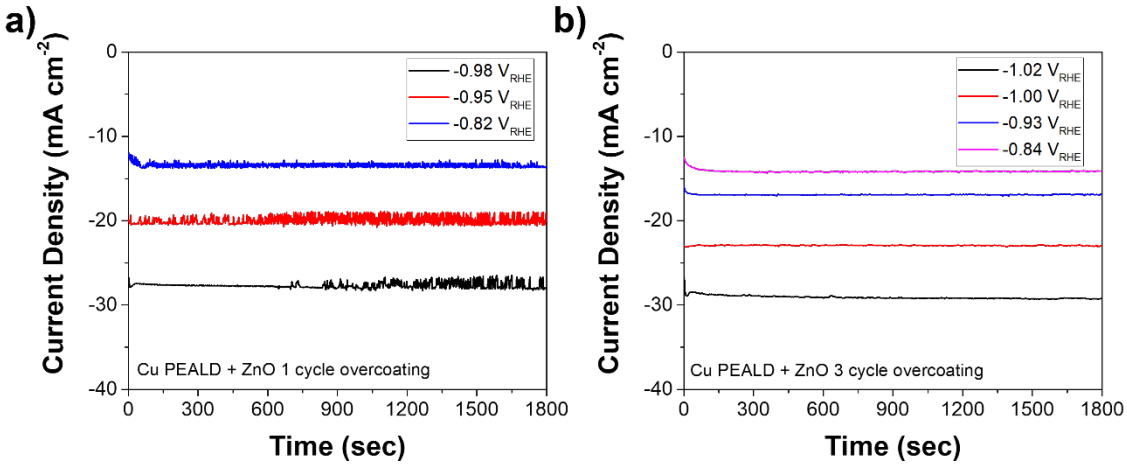

Figure S10. Representative total current density of ZnO 1 cycle and 3 cycle overcoating on Cu PEALD catalysts for each applied potential. a) Total current density of ZnO 1 cycle overcoating catalyst. b) Total current density of ZnO 3 cycle overcoating catalyst.

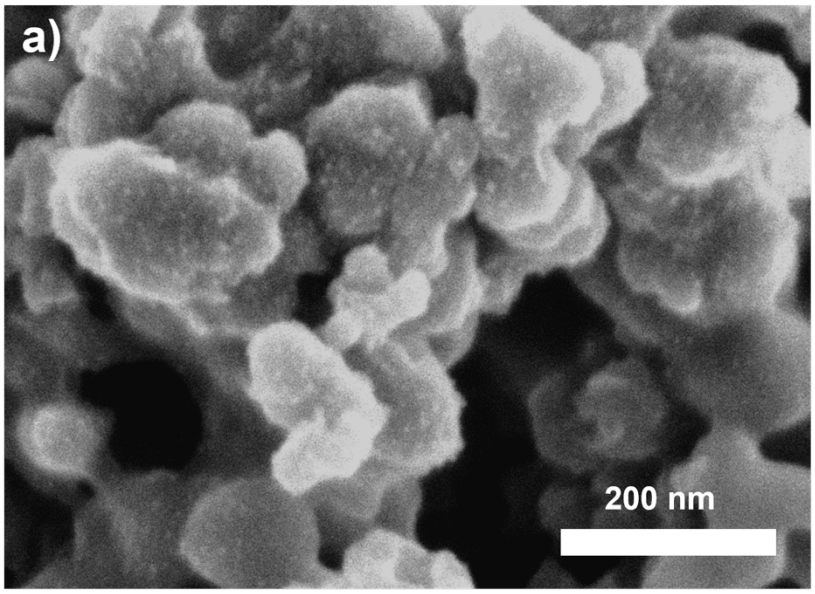

Figure S11. SEM image after 1 cycle Al_2O_3 ALD overcoating on 510 cycles Cu PEALD NP catalyst.

Table S2. Elemental percentage results of ZnO 1 cycle, ZnO 3 cycle and Al_2O_3 1 cycle overcoating on Cu PEALD catalysts using XPS.

Element	ZnO ALD 1 cycle (At %)	ZnO ALD 3 cycle (At %)	Al_2O_3 ALD 1cycle (At %)
Cu	2.12	1.37	2.92
Zn	1.11	1.05	-
Al	-	-	11.90
C	79.68	76.06	66.33
O	4.76	4.81	7.86
F	12.33	16.70	10.99

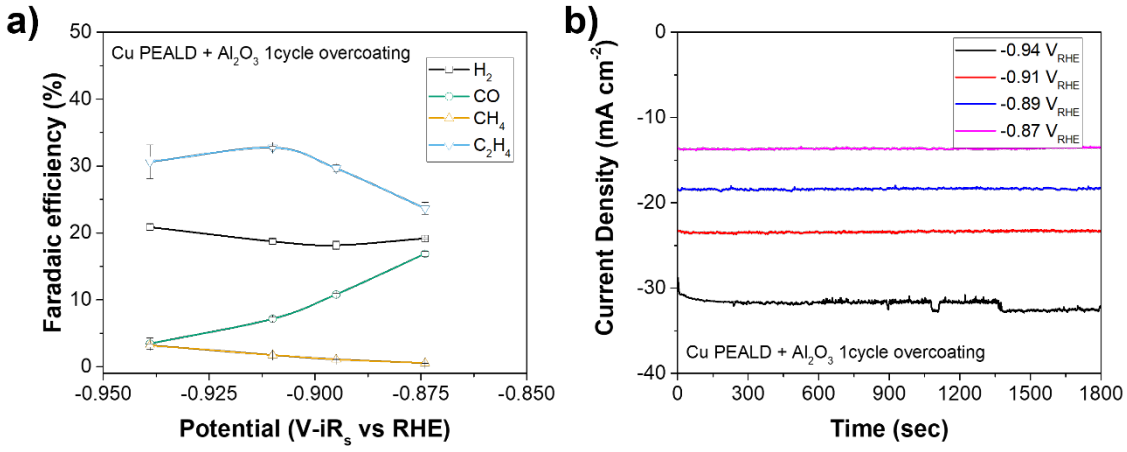

Figure S12. Potential-dependent Faradaic efficiency of gaseous products and representative total current density results for Al_2O_3 1 cycle overcoating on Cu PEALD catalyst. a) Potential-dependent Faradaic efficiency result of Al_2O_3 1 cycle overcoating on Cu PEALD catalyst. b) Representative total current density results of Al_2O_3 1 cycle overcoating on Cu PEALD catalyst for each applied potential.

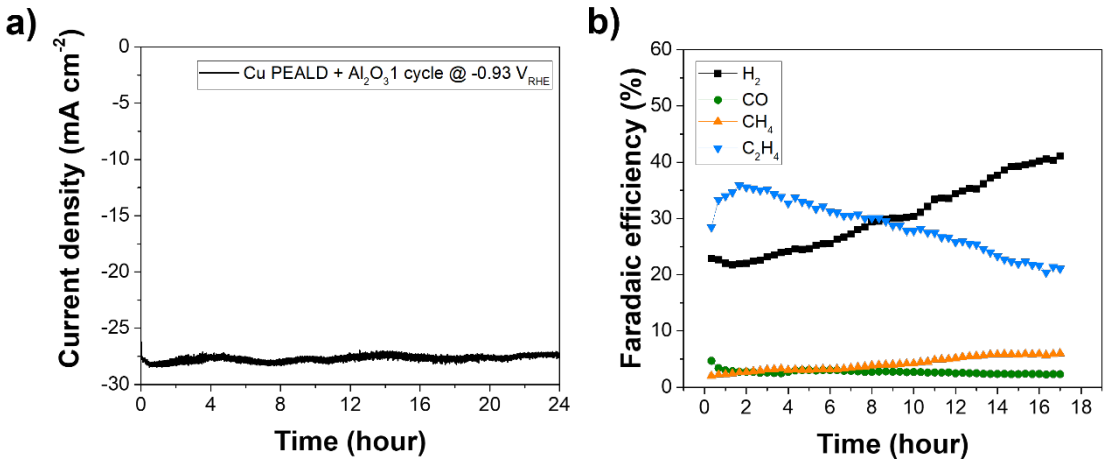

Figure S13. ECR stability measurement results of Al_2O_3 1 cycle over coating on Cu PEALD catalyst at -0.93 V vs. RHE. a) Current density results over 24 hours. b) Faradaic efficiency changes of gaseous products over 17 hours.

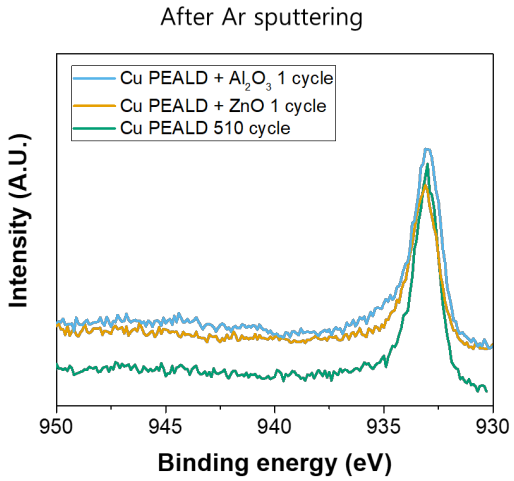

Figure S14. Comparison of Cu 2p XPS spectra of a pristine Cu PEALD catalyst, 1 cycle ZnO ALD overcoat, and 1 cycle Al2O3 ALD overcoat, after 1 min Ar sputtering.

References

1. J. D. Lenef, S. Y. Lee, K. M. Fuelling, K. E. Rivera Cruz, A. Prajapati, D. O. Delgado Cornejo, T. H. Cho, K. Sun, E. Alvarado, T. S. Arthur, C. A. Roberts, C. Hahn, C. C. L. McCrory, and N. P. Dasgupta, *Nano Lett.*, 2023, **23**, 10779–10787
2. N. P. Dasgupta, J. F. Mack, M. C. Langston, A. Bousetta, F. B. Prinz, *Rev. Sci. Instrum.* 2010, **81**, 44102.